Journal of The Electrochemical Society, **151** (3) B188-B194 (2004)
0013-4651/2004/151(3)/B188/7/$7.00 © The Electrochemical Society, Inc.

Effect of Heat-Treatment on Characteristics of Anodized Aluminum Oxide Formed in Ammonium Adipate Solution

Jeng-Kuei Chang,[a] Chia-Mei Lin,[a] Chi-Min Liao,[b] Chih-Hsiung Chen,[b] and Wen-Ta Tsai[a,*,z]

[a]*Department of Materials Science and Engineering, National Cheng Kung University, Tainan, Taiwan*
[b]*China Steel Corporation, New Materials Research and Development Department, Kaoshiung, Taiwan*

The effects of heat-treatment (before and after anodization) on the microstructure and electrochemical characteristics of anodized aluminum oxide films formed in 85°C aqueous ammonium adipate electrolyte were investigated. The morphology and crystal structure of the anodized oxide were examined by transmission electron microscopy. The capacitance, relative dielectric constant, electrochemical impedance spectroscopy, and I-V behavior of the oxide film were also determined. Both pre- and post-heat-treatment at 500°C could induce the formation of crystalline γ'-Al_2O_3 in the outer layer of anodized oxide and consequently increase the relative dielectric constant of the film. The differences in the morphology and crystalline characteristics between the anodized oxide subjected to pre- and/or post-heat-treatments led to variations in the electrochemical properties. The pre-heat-treatment could economize the required charge to anodize the oxide and retard the growth of film thickness during anodizing. Thermal-induced phase transformation from amorphous to crystalline oxide of the anodized film due to post-heat-treatment, could leave some defects and substantially decrease the electrical resistance of the oxide layer. The reanodization further developed and extended the crystalline oxide formation, which subsequently increased the relative dielectric constant of the oxide film.
 [DOI: 10.1149/1.1646140]

Manuscript submitted February 27, 2003; revised manuscript received October 10, 2003. Available electronically February 5, 2004.

Barrier aluminum oxide finds many applications in the integrated circuit process,[1] thin film transistor/liquid crystal display fabrication,[2] metal-insulator-metal cathodes for electron-beam lithography, and electrolytic capacitors.[3] Depending on the anodizing conditions, either amorphous or crystalline barrier aluminum oxide can be formed. Because the crystalline oxide can sustain a higher voltage,[4] has a higher relative dielectric constant,[5,6] and possesses a lower ionic conductivity than that of the amorphous oxide film, work on developing an anodized film with a high degree of crystallinity is of continuous interest to researchers.[7] Crystalline oxide growth may be promoted by the presence of a thin layer of thermal oxide on the surface of aluminum.[5,8-12] The thermal oxide, which contains γ-Al_2O_3[13,14] crystals, becomes incorporated into the growing barrier oxide and acts as nuclei for the amorphous to γ'-Al_2O_3 transformation.[10,11] But the development, during the anodization, of γ'-Al_2O_3 within the anodized oxide film formed on aluminum covered with a thin thermal oxide is strongly influenced by the nature of the anion species of the electrolytes.[15] Although the film morphology, crystalline characteristics, and growing mechanism of dielectric oxides anodized in borate and phosphate electrolytes had been extensively reported,[10-12,15-17] those formed in ammonium adipate solution, a common medium to anodize the aluminum for use in low-voltage electrolytic capacitors, were rarely explored.

In a recent study, the dependence of the microstructure of aluminum anodized film on the forming voltage in ammonium adipate solution has been elucidated.[6] Whether the heat-treatment before the anodizing process in ammonium adipate solution affects the transition from amorphous to crystalline form for the anodized film is of interest and is studied here. Furthermore, because post-heat-treatment and reanodization are common practices in the fabrication of an anodized aluminum foil for electrolytic capacitors, the effects of post-heat-treatment and reanodization on the crystalline characteristics as well as the electrochemical performance of the anodized oxide are also examined in this work.

Experimental

Specimens 10 cm^2 in area were cut from 100 μm thick, O-temper, 99.99% aluminum foil containing 0.0028 Fe, 0.0033 Si, and 0.0016 wt % Cu. All specimens were washed in HNO_3 + Na_2SO_4 solution at 80°C for 2 min to remove the oxide and the grease on the sample surface, then rinsed thoroughly in deionized water, and finally dried in a warm airstream. Some of the cleaned aluminum foils were heat-treated in air at 500°C for 30 min. The cleaned and the preheat-treated specimens were than anodized in ammonium adipate solution (150 g/1000 g H_2O) at 85°C. A 304 stainless steel (SS) plate was used as the counter electrode. A constant current density of 25 mA/cm^2 was passed through the cell between the aluminum sample and the counter electrode until the potential difference reached 100 V. Then, the voltage was held for 10 min, and the current was allowed to decay. During the anodization, the variation of the current density with time (i-t curve) was recorded. Post-heat-treatments at 500°C for 30 min were applied to some of the anodized specimens. Among the anodized specimens, some were further reanodized using the same process except for a holding time shortened to 2 min in the controlled-potential stage. The preceding conditions for specimen preparation are listed in Table I.

The ultrathin sectioning technique[18,19] was employed to prepare the cross-sectional samples of the anodized aluminum foils for the transmission electron microscopy (TEM) analysis. Anodized specimens were first cut into strips about 0.1 × 20 mm. These strips were then placed vertically in gelatin capsules containing Spurr's epoxy resin mix. The capsules were kept under reduced pressure by an aspirator. This allowed the resin to fully penetrate the surface of each specimen. The samples were then kept at 60°C over 24 h for complete polymerization. The blocks of resin were trimmed initially with a steel knife and sectioned with the diamond knife of an ultramicrotome. The cutting direction was parallel to the metal/film interface, and the section thickness was generally 40-60 nm. The sections were mounted on copper grids and examined in a transmission electron microscope at 200 kV. A camera length of 100 cm was adopted as the nanobeam electron diffraction was performed.

The capacitance of the various anodized oxide films in 25°C aqueous ammonium adipate solution (150 g/1000 g H_2O) was measured using a typical LCR meter. A pure aluminum sheet with a very large area was used as the counter electrode. The perturbation was 1.2 V_{rms} at 120 Hz.

Electrochemical impedance spectroscopy (EIS) was also carried out to investigate the electrochemical characteristics of the anodized oxide film. The test cell was a three-electrode system with the anodized aluminum assembled as the working electrode. A platinum sheet and a saturated calomel electrode were used as the counter electrode and the reference electrode, respectively. The latter employed a salt bridge with a probe adjacent to the working electrode.

* Electrochemical Society Active Member.
z) E-mail: wttsai@mail.ncku.edu.tw

Table I. Conditions for anodization and heat-treatment for preparations of aluminum oxide in ammonium adipate solution.

Designation\Condition	Pre-heat-treatment	Anodization	Post-heat-treatment	Reanodization
A	NA	85°C, 10 min	NA	NA
B	NA	85°C, 10 min	NA	85°C, 2 min
C	500°C, 30 min, in air	85°C, 10 min	NA	NA
D	500°C, 30 min, in air	85°C, 10 min	NA	85°C, 2 min
E	NA	85°C, 10 min	500°C, 30 min, in air	NA
F	NA	85°C, 10 min	500°C, 30 min, in air	85°C, 2 min

The testing solution was also a 25°C aqueous ammonium adipate solution (150 g/1000 g H_2O). An EG&G model 263 potentiostat connected to a Solartron 1255 frequency response analyzer was used for the electrochemical measurement. The input voltage signal had an amplitude of 10 mV_{rms} at open-circuit potential and typically scanned from 100 kHz to 5 MHz.

The current-voltage (I-V) curves of the various anodized aluminum electrodes were measured by a sourcemeter (Keithley 2400). The voltage scanning rate was 2 V per second, and the variation of the current was recorded. The test was performed in 25°C aqueous ammonium adipate solution (150 g/1000 g H_2O), and a 304 SS plate was used as the counter electrode.

Results and Discussion

Morphology and microstructure of the anodized oxide films.—Figure 1a shows the cross-sectional morphology of the aluminum foil anodized at 100 V in 85°C ammonium adipate solution (condition A). A barrier oxide film, about 165 nm thick, was clearly identified on top of the aluminum substrate as a grayish band. The crystal structure of the anodized oxide film was examined by electron diffraction. Figure 1b presents the analytic result, indicating the amorphous nature of the anodized oxide. The morphology and crystal structure of the oxide layer subjected to reanodization treatment (condition B) were similar to those revealed in Fig. 1. But the thickness of the amorphous oxide film increased slightly to about 170 nm.

The TEM bright-field image of the anodized oxide film formed on the pre-heat-treated aluminum surface (condition C) is shown in Fig. 2a. The image shows that the oxide consisted of two distinct zones. Nanobeam electron diffraction analysis indicated the presence of a crystalline outer layer on top of the inner amorphous anodized oxide. The nanobeam electron diffraction patterns of the outer layer of crystalline oxide, with (001), (011), and (111) poles, are shown in Fig. 2b, c, and d, respectively. The analytic result confirmed that the oxide was γ'-Al_2O_3.[20] Clearly, pre-heat-treatment at 500°C for 30 min assisted the formation of crystalline oxide in the anodized film. It has been reported that the thermally formed crystalline γ-Al_2O_3 could act as the nucleation site for forming γ'-Al_2O_3 in Al anodizing.[10,11] The presence of the outer layer of crystalline γ'-Al_2O_3, as revealed in Fig. 2a, was probably associated with the thermal oxide formed during pre-heat-treatment. It has been shown that the aluminum oxide film grew by both outward diffusion of aluminum ions and inward diffusion of oxygen ions during the anodization.[21,22] The layered structure observed in Fig. 2a may thus be explained as follows. In the presence of γ-Al_2O_3, the outward diffusion of Al^{3+} resulted in the formation of γ'-Al_2O_3 on the γ-Al_2O_3 nuclei, while the inward diffusion of O^{2-} caused the formation of amorphous oxide at the γ-Al_2O_3/Al substrate interface. As the anodization process continued, two distinct layers of oxide, with one crystalline outer layer and another amorphous inner layer, thus developed.

Thorough examination of the TEM image showed that the crystalline γ'-Al_2O_3 was not uniform. Some region of the anodized oxide was completely amorphous throughout the whole thickness. This observation suggested that the surface was not completely covered by γ-Al_2O_3 after pre-heat-treatment at 500°C for 30 min. The thickness of the anodized film in the region without crystalline oxide was greater than that with an outer crystalline layer. This observation suggested that ionic diffusion in the amorphous oxide was faster than in the crystalline oxide. In general, the average anodized film thickness was about 150 nm, which was thinner than that of the film anodized on the Al foil without pre-heat-treatment (condition A). Clearly, the presence of thermal oxide on the aluminum electrode could retard the growth of the aluminum oxide film during the anodization.

Figure 3 shows the TEM micrograph of the reanodized oxide film formed on the pre-heat-treated Al surface (condition D). The reanodization treatment caused a slight increase in the average oxide film thickness (155 nm) compared to that of condition C. The outer

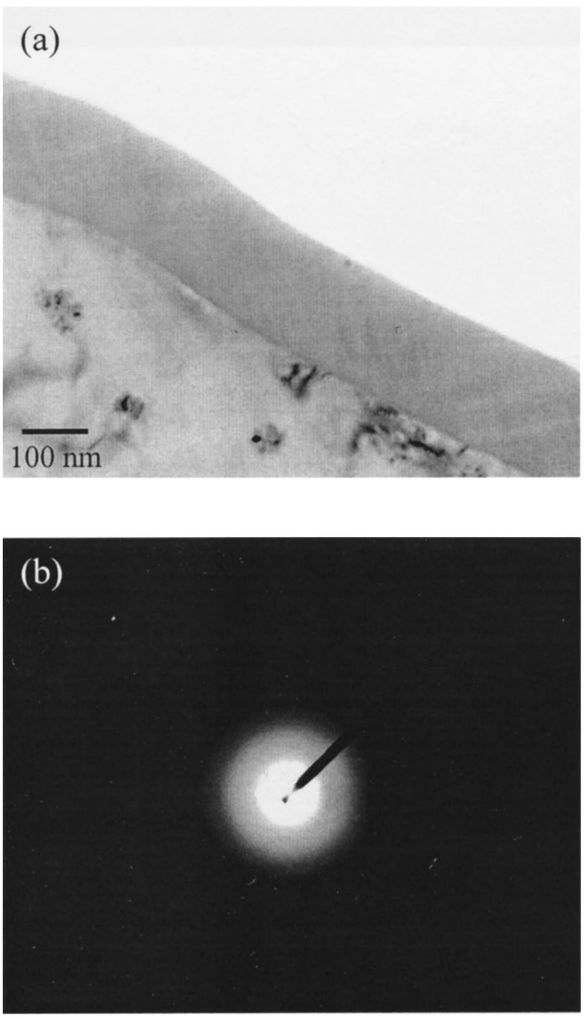

Figure 1. (a) TEM cross-sectional image of the aluminum foil anodized at 100 V in 85°C ammonium adipate solution (condition A), (b) electron diffraction pattern taken from the oxide film.

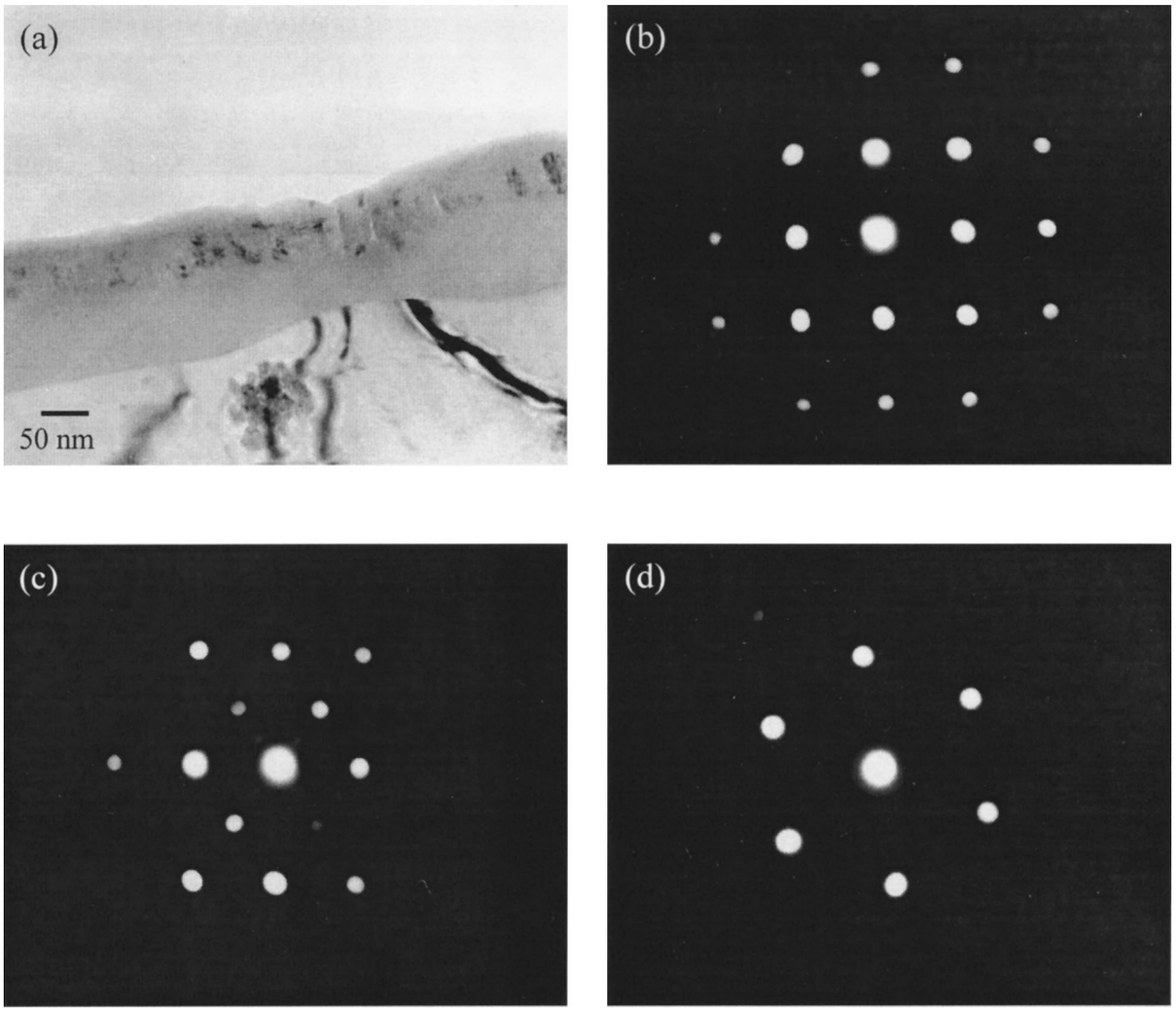

Figure 2. (a) TEM cross-sectional image of the anodized oxide film formed on the pre-heat-treated aluminum surface (condition C). (b), (c), and (d) Electron diffraction patterns taken from the (001), (011), and (111) poles of the crystalline region.

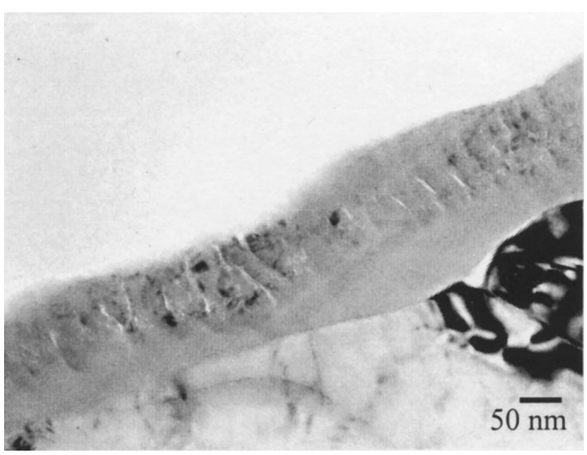

Figure 3. TEM cross-sectional image of the reanodized oxide film formed on the pre-heat-treated Al surface (condition D).

crystalline layer extended, whereas the thickness of the inner amorphous layer remained almost unchanged. It seemed that the inward diffusion of O^{2-} to form amorphous oxide was retarded by the existing external crystalline oxide. However, the outward diffusion of Al^{3+} to form crystalline oxide did not slow down in the amorphous zone. As a result, the outer layer of crystalline oxide had a relatively slight increase in thickness.

For the specimen prepared according to condition E, the cross-sectional morphology is demonstrated in Fig. 4. An obvious change in the TEM image was noticed, as compared with that shown in Fig. 1. The image shown in Fig. 4 exhibited an outer layer with dispersed crystalline oxide and an inner amorphous oxide layer. The crystal structure and their distributions were identified by electron diffraction analyses. The crystalline oxide formed in the outer layer after post-heat-treatment was confirmed to be γ'-Al_2O_3. The results demonstrated that post-heat-treatment could induce amorphous-to-crystalline transformation for the anodized oxide. Interestingly, the heat-treatment-induced crystalline formation occurred in the outer layer, not in the inner layer, of the anodized film. More work is needed in the future to clarify the selective transformation behavior of the heat-treated anodized oxide. For the specimen prepared following the process of condition E, the oxide layer was about 175 nm thick. This implied that further thickening of the oxide film occurred during post-heat-treatment at 500°C for 30 min. Moreover, the re-

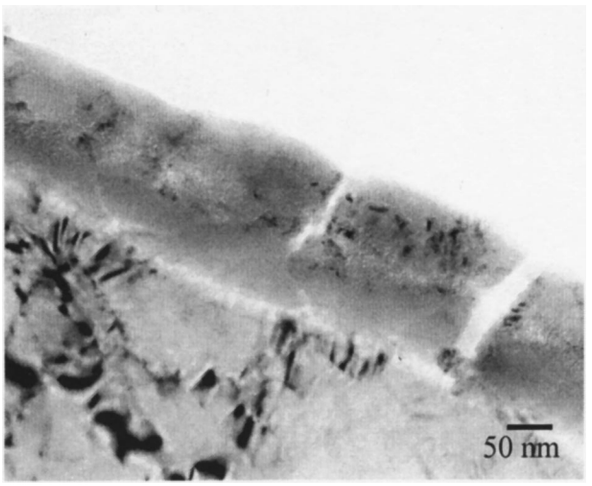

Figure 4. TEM cross-sectional image of the anodized oxide film subjected to post-heat-treatment at 500°C for 30 min (condition E).

sults from electron diffraction analysis indicated that the crystalline oxide formed during post-heat-treatment was γ'-Al_2O_3 rather than γ-Al_2O_3.

Reanodizing of the post-heat-treated anodized film (condition F) gave rise to a more complicated microstructure, as shown in Fig. 5. The TEM image shown in Fig. 5 seemed to reveal that a continuous layer of crystalline oxide formed between an outer layer in which the crystalline phase dispersed in the amorphous substrate and an inner amorphous layer. As mentioned earlier, the amorphous phase would provide an easy path for both Al^{3+} and O^{2-} diffusion. Because the outer layer of the post-heat-treated anodized film consisted of amorphous oxide with dispersed γ'-Al_2O_3, there still existed an easy diffusion channel between crystalline oxide particles in the outer layer. By holding the voltage at 100 V for 2 min during the reanodizing treatment, the almost equal flux of Al^{3+} and O^{2-} could reach a position near the center of the anodized film. Consequently, the growth of the already existing γ'-Al_2O_3 became favored, and a continuous layer of γ'-Al_2O_3 was formed. Because the holding time at 100 V was only 2 min, this crystalline oxide layer did not grow

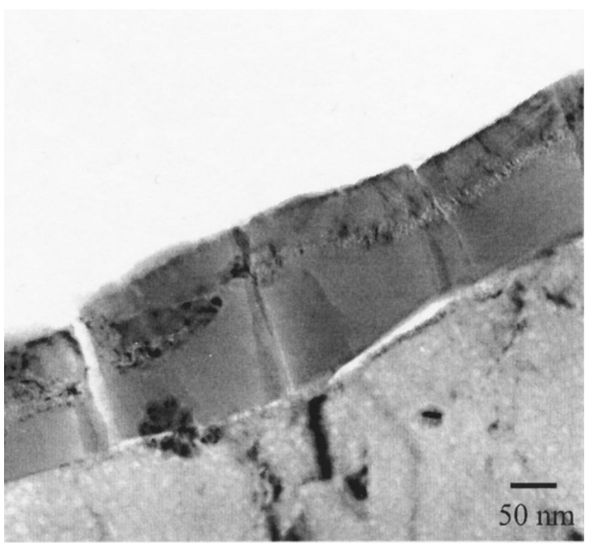

Figure 5. TEM cross-sectional image of the post-heat-treated oxide film subjected to reanodization process (condition F).

Table II. Capacitance, thickness, and relative dielectric constant of the anodized oxide films formed under various conditions.

Anodizing condition	C [a] (nF/cm^2)	d (nm)	Relative dielectric constant
A	62.3	165	11.6
B	60.5	170	11.6
C	79.3	150	13.4
D	81.0	155	14.2
E	61.3	175	12.1
F	60.9	180	12.4

[a] The capacitance is measured by the LCR meter at a frequency of 100 Hz.

throughout the whole thickness. As a result, the complicated microstructure revealed in Fig. 5 consisted of an inner amorphous and intermediate continuous γ'-Al_2O_3 and an outer crystalline dispersed amorphous layer. Obviously, reanodizing could contribute to the oxide film thickening process. The average oxide film thickness of the specimen prepared according to condition F was 180 nm. The average oxide film thicknesses of all the specimens examined are listed in Table II.

As revealed in Fig. 2-5, cracks or defects were formed in the anodized film, particularly in the regions containing the crystalline phase. Post-heat-treatment further increased the amount of defects formed in the anodized oxide film and subsequently increased the brittleness of the oxide. The through-film-thickness cracks shown in Fig. 4 and 5, formed during cutting and ultramicrotomy for TEM specimen preparation, were believed due to the increase of film brittleness.

The charge required to form the anodized oxide layer.—The variations of current density and potential with time were recorded during anodizing. Figure 6 plots the changes of potential and the anodizing current densities at the initial stage (0-50 s) for the aluminum foil, illustrating the effect of pre-heat-treatment (500°C in air, for 30 min). As seen in this figure, it took about 7 and 10 s, respectively, for the specimens with and without pre-heat-treatment to reach the defined voltage (100 V) under a constant-current (25 mA/cm^2) condition. Then the anodizing process was switched to voltage-control mode. As shown in Fig. 6, the current density immediately decreased as soon as the control mode was changed. The charge required to form the anodized oxide layer with or without the thermal oxide on the aluminum, evaluated by integrating the ob-

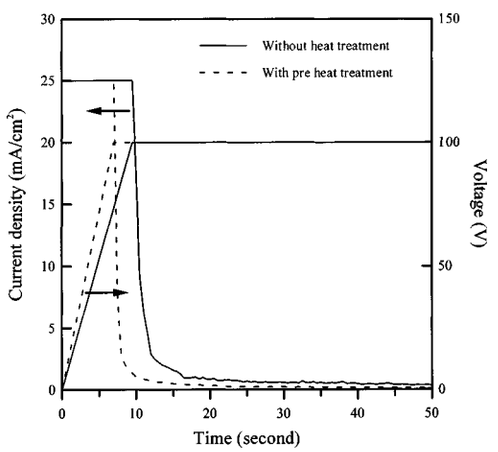

Figure 6. The variations of current density and potential with time during the initial stage of anodization in 85°C aqueous ammonium adipate electrolyte (150 g/1000 g H_2O) for the aluminum foil with and without pre-heat-treatment.

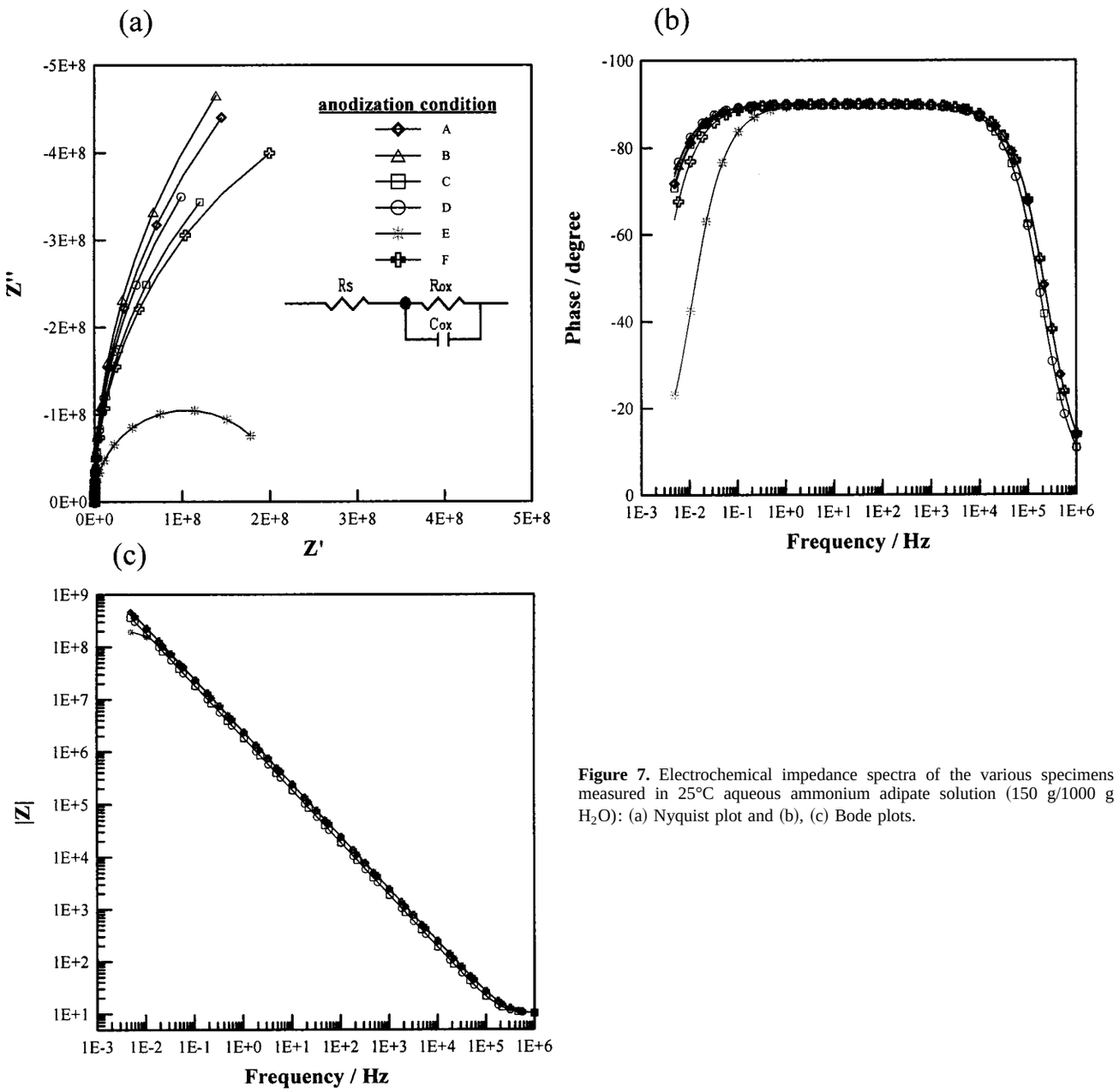

Figure 7. Electrochemical impedance spectra of the various specimens measured in 25°C aqueous ammonium adipate solution (150 g/1000 g H_2O): (a) Nyquist plot and (b), (c) Bode plots.

tained i-t curves during anodizing (10 min), was 225 and 300 mC/cm^2, respectively. Clearly, there was about 25% charge economized to form the anodized oxide film when the aluminum foil was pre-heat-treated at 500°C in air for 30 min. The reduction of required charge to form the anodized oxide film due to the presence of thermal oxide well agreed with the previous reports,[10,12] in which the aluminum foils were anodized in electrolytes other than ammonium adipate solution.

Relative dielectric constant of the anodized oxide films.—The capacitances, measured in ammonium adipate solution by a typical LCR meter, of the anodized aluminum oxides formed in various conditions are listed in Table II. The capacitance (C) can be expressed by the following equation

$$C = \varepsilon_o \varepsilon_r a/d$$

where ε_o represents the dielectric constant in vacuum (8.854 $\times$ 10^{-12} F/m), ε_r is the relative dielectric constant of the anodized oxide film, a is the area of the electrode, and d is the thickness of the dielectric layer. For a given a and with d measured from the TEM micrograph, the relative dielectric constant of each anodized oxide film can be calculated. The results calculated for various anodized oxides are also listed in Table II. For conditions A and B, the relative dielectric constants of the anodized oxide films were the same (11.6). In both cases, the anodized oxides were amorphous. When pre-heat-treatment was applied, as for conditions C and D, the relative dielectric constants of the anodized film increased. The presence of γ'-Al_2O_3 in the anodized film was the main factor for the high relative dielectric constant observed. Under anodizing condition D, the amount of γ'-Al_2O_3 in the anodized film was more than that anodized under condition C (as discussed in the previous section); therefore, the relative dielectric constant of the former was higher than that of the latter. Although post-heat-treatment could cause the transformation of amorphous oxide to crystalline oxide, lower val-

Table III. The capacitance (C_{OX}) and resistance (R_{OX}) of the anodized oxide films obtained from EIS analyses.

	C_{OX} (nF/cm^2)	R_{OX} (MΩ cm^2)
Specimen A	65.2	1480
Specimen B	62.8	1700
Specimen C	82.5	1100
Specimen D	84.3	1350
Specimen E	64.5	210
Specimen F	63.7	1000

ues of relative dielectric constants for the anodized films prepared according to conditions E and F (as compared to those of conditions C and D) were found. The change of the relative dielectric constants was probably due to the difference in distribution of crystalline γ'-Al_2O_3 within the anodized films. The relatively higher values of the relative dielectric constants observed for the reanodized oxides, for both pre- and post-heat-treated specimens, were attributed to the higher amount of γ'-Al_2O_3 in the film.

Electrochemical characteristics of the anodized oxide films.—Figure 7 shows the results of EIS measurements conducted in ammonium adipate solution (150 g/1000 g H_2O) for the various anodized aluminum specimens. As seen in this figure, capacitive behavior was dominant over the frequency range considered in this investigation for all the electrodes with different forming conditions. The impedance data presented in terms of a Nyquist plot (Fig. 7a) or Bode plots (Fig. 7b and c) all indicated that these electrodes could be simulated by an equivalent circuit with a single time constant, as demonstrated in the inset of Fig. 7a. The equivalent circuit consisted of a parallel combination of the oxide film resistance (R_{OX}) and capacitance (C_{OX}), connected in series to a solution resistance (R_S). With this equivalent circuit and the impedance spectrum obtained, the resistances and the capacitances of the anodized aluminum oxide films formed at various conditions could be evaluated. The results are listed in Table III. The magnitudes of the capacitances determined using EIS generally agreed with those determined by LCR meter under a fixed frequency of 100 Hz (Table II). The effect of anodizing condition on the change of capacitance could also be resolved using both EIS and LCR methods, and the results agreed well each other.

As can be seen in Table III, the resistance of the amorphous oxide film was higher than that containing crystalline oxide. The defects induced from the crystallization of γ'-Al_2O_3 caused a decrease in the film resistance (R_{OX}). Post-heat-treatment rendered the anodized film with an increasing amount of defects in the oxide and consequently gave rise to the lowest film resistance (210 MΩ cm^2). However, the reanodizing treatment could help to seal the defects induced by crystallization of amorphous oxide to form γ'-Al_2O_3, resulting in a recovery of the film resistance. The effect of reanodizing treatment on repairing the defects in the anodized film containing crystalline γ'-Al_2O_3 was also recognized for the pre-heat-treated specimen (comparing conditions C and D).

Figure 8 plots the I-V curves of the anodized aluminum electrodes determined in ammonium adipate solution (150 g/1000 g H_2O) at 25°C, and at a potential sweeping rate of 2 V/s. The curves in Fig. 8 demonstrate that the current density increased gradually with increasing potential until an abrupt transition. Before the transition occurred, the current detected is considered as the leakage current. The higher leakage currents observed for curves E and F were consistent with the lower oxide resistance as determined in EIS analyses (see Table III). Clearly, post-heat-treatment would lower the oxide resistance by forming crystallization-induced defects. As seen in Fig. 8, the reanodization process would lower the leakage current of the anodized films (by comparing curves A, C, and E with curves B, D, and F, respectively). The beneficial effect of reanodization in repairing the defects within the anodized film was clearly demonstrated. The occurrence of transition, or the abrupt increase in

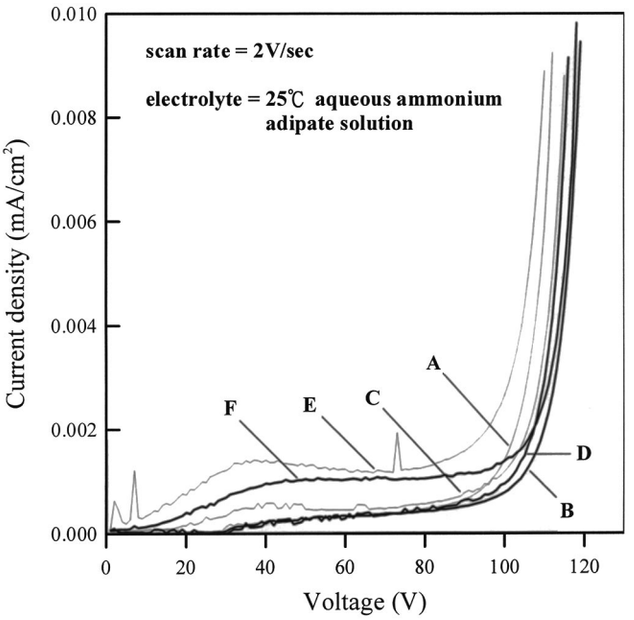

Figure 8. The I-V curves of the anodized aluminum specimens.

current density, is associated with the breakdown of the dielectric oxide layer. Therefore, the transition potential could be used to evaluate the stability of the anodized oxide. For comparison, the transition voltage was determined from the I-V curve at the point where the slope equaled 1×10^{-4} (mA/cm^2)/V. In this investigation, the transition voltages were close to the forming voltage (*i.e.*, 100 V). For the specimen anodized according to condition A, the transition voltage was 98 V, which was lower than that anodized according to condition C (102 V). This implied that pre-heat-treatment would lead to the formation of a more stable anodized oxide. As pointed out earlier, crystalline oxide, γ'-Al_2O_3, was formed when applying pre-heat-treatment. The higher transition voltage determined in case C, compared to that in case A, was probably associated with the existence of crystalline oxide in the anodized film. The lowest transition voltage (95 V) was found in case E. This anodized film (post-heat-treated but without reanodization) contained a relatively higher density of defects. The stability of this anodized film thus deteriorated. Furthermore, the transition voltages for the reanodized oxide (conditions B, D, and F) were all higher than those without reanodization treatment (conditions A, C, and E). This observation indicated that reanodization improved the oxide film stability.

Conclusions

The effects of heat-treatment and reanodization on the morphology, crystal structure, and electrochemical properties of anodized aluminum oxide films formed in 85°C aqueous ammonium adipate electrolyte (150 g/1000 g H_2O) are summarized as follows.

1. Pre-heat-treatment could economize the required charge to form the aluminum anodized film and induce the formation of the crystalline γ'-Al_2O_3 in oxide. The anodized film consisted of two distinct zones: an outer crystalline layer and an inner amorphous layer. The presence of thermal oxide on the aluminum foil (formed during pre-heat-treatment) could retard the growth of the oxide during the anodization and consequently decrease the film thickness.

2. Post-heat-treatment could induce amorphous-to-crystalline transformation in the outer layer of the anodized oxide. An outer layer with dispersed γ'-Al_2O_3 crystalline oxide and an inner amorphous oxide layer were observed in the TEM micrograph. The defects induced from the crystallization of γ'-Al_2O_3 would significantly decrease the film resistance and deteriorate the stability of the

anodized oxide. When the oxide was subjected to reanodization, an intermediate continuous layer of crystalline oxide formed within the film.

3. The presence of the crystalline γ'-Al_2O_3 within the anodized oxide could increase the relative dielectric constant of film. The higher value of the relative dielectric constants observed for the pre-heat-treated and reanodized oxides were attributed to the higher amount of γ'-Al_2O_3 in the film.

4. Reanodization process of the aluminum oxide could extend the crystalline γ'-Al_2O_3 within the film and help to seal the defects induced by crystallization of amorphous oxide. This process resulted in an improved electrical resistance and stability of the anodized oxide film.

National Cheng Kung University assisted in meeting the publication costs of this article.

References

1. R. L. Chiu, P. H. Chang, and C. H. Tung, *J. Electrochem. Soc.*, **142**, 525 (1995).
2. A. Delong and V. Kolarik, *J. Vac. Sci. Technol. B*, **7**, 1422 (1989).
3. R. W. Franklin, in *Proceedings of a Conference on Anodizing*, p. 96, Aluminum Development Association, London (1962).
4. R. S. Alwitt and H. Takei, *Thin Films Sci. Technol.*, **4**, 741 (1983).
5. W. J. Bernard and S. M. Florio, *J. Electrochem. Soc.*, **132**, 2319 (1985).
6. J. K. Chang, C. M. Liao, C. H. Chen, and W. T. Tsai, *J. Electrochem. Soc.*, **150**, B266 (2003).
7. H. Uchi, T. Kanno, and R. S. Alwitt, *J. Electrochem. Soc.*, **148**, B17 (2001).
8. R. S. Alwitt and H. Takei, in *Passivity of Metals and Semiconductors*, M. Froment, Editor, p. 741, Elsevier Science Publishers, Amsterdam (1983).
9. C. Crevecoeur and H. J. de Wit, Paper 132 presented at the 27th Meeting of the International Society of Electrochemistry, Zurich (1976).
10. C. T. Chen and G. A. Hutchins, *J. Electrochem. Soc.*, **132**, 1567 (1985).
11. K. Kobayashi, K. Shimizu, and H. Nishibe, *J. Electrochem. Soc.*, **133**, 140 (1986).
12. C. Crevecoeur and H. J. de Wit, *J. Electrochem. Soc.*, **134**, 808 (1987).
13. A. F. Beck, M. A. Heine, E. J. Caule, and M. J. Pryor, *Corros. Sci.*, **7**, 1 (1967).
14. P. E. Doherty and R. S. Davis, *J. Appl. Phys.*, **34**, 619 (1963).
15. K. Kobayashi, K. Shimizu, and D. Teranishi, *Jpn. J. Inst. Light Met.*, **36**, 81 (1986).
16. K. Kobayashi and K. Shimizu, *J. Electrochem. Soc.*, **135**, 908 (1988).
17. H. Takahashi, M. Dairaku, and M. Seo, *J. Met. Finish. Soc. Jpn.*, **45**, 60 (1994).
18. K. Shimizu, G. M. Brown, K. Kobayashi, P. Skeldon, G. E. Thompson, and G. C. Wood, *Corros. Sci.*, **40**, 1049 (1998).
19. R. C. Furneaux, G. E. Thompson, and G. C. Wood, *Corros. Sci.*, **18**, 853 (1978).
20. E. J. W. Verwey, *J. Chem. Phys.*, **3**, 592 (1935).
21. K. Shimizu, G. E. Thompson, G. C. Wood, and Y. Xu, *Thin Solid Films*, **88**, 255 (1982).
22. K. Shimizu, G. M. Brown, H. Habazaki, K. Kobayashi, P. Skeldon, G. E. Thompson, and G. C. Wood, *Electrochim. Acta*, **44**, 2297 (1999).